

# Rotation-Induced Breakdown of Torsional Quantum Control

L. H. Coudert\*

*Laboratoire Inter-universitaire des Systèmes Atmosphériques, UMR 7583 du CNRS, Universités Paris Est Créteil et Paris Diderot, 61 Avenue du Général de Gaulle, 94010 Créteil Cedex, France*

Luis F. Pacios

*Unidad de Química y Bioquímica, Departamento de Biotecnología, ETSI Montes, Universidad Politécnica de Madrid, 28040 Madrid, Spain*

Juan Ortigoso†

*Instituto de Estructura de la Materia, CSIC, Serrano 121, 28006 Madrid, Spain*

Control of the torsional angles of nonrigid molecules is key for the development of emerging areas like molecular electronics and nanotechnology. Based on a rigorous calculation of the rotation-torsion-Stark energy levels of nonrigid biphenyl-like molecules, we show that, unlike previously believed, instantaneous rotation-torsion-Stark eigenstates of such molecules, interacting with a strong laser field, present a large degree of delocalization in the torsional coordinate even for the lowest energy states. This is due to a strong coupling between overall rotation and torsion leading to a breakdown of the torsional alignment. Thus, adiabatic control of changes on the planarity of this kind of molecule is essentially impossible unless the temperature is on the order of a few Kelvin.

Quantum control of molecular degrees of freedom is becoming an important field of research that promises important technological developments. In the last few years impressive progress on the control of molecular alignment and orientation has been achieved [1]. However, control of internal degrees of freedom remains in its infancy due, among other things, to the elusive character of intramolecular vibrational relaxation processes which are prevalent even in relatively small polyatomic molecules. Quantum control of a large amplitude torsional angle has been the subject of several recent investigations [2–7].

Control of torsional angles is key for the development of new miniaturized communication systems based on energy transfer along molecular wires [2,3]. For example, it has been established that the rate of electron exchange in a ruthenium (II)-osmium (II) binuclear complex depends on the conformation of a biphenyl bridge [4]. Ramakrishna and Seideman [5] showed that torsional control by an intense laser pulse should be achieved for several nonrigid molecules displaying internal rotation. In the case of biphenyl, using a model where the two phenyl rings can rotate about a fixed axis perpendicular to the direction along which the laser field is propagating, their calculation predicts that the two rings become localized in the same plane for a circularly polarized laser field of intensity around  $10^{10}$  W/cm<sup>2</sup> and temperatures up to 77 K. In their time dependent experiments, Madsen and co-workers [6,7] showed that for the similar 3, 5-difluoro-3', 5'-dibromobiphenyl molecule, torsional control of the internal rotation

can be achieved using two laser pulses. The first pulse adiabatically aligns the C-C bond between the phenyl rings along its polarization axis. The second pulse imparts a kick to the molecule that is able to initiate torsional motion. These experimental results were corroborated [6,7] using a theoretical model analogous to that of Ref. [5].

In conventional spectroscopic studies, large amplitude motions have been traditionally difficult to analyze due to the existence of strong couplings with the overall rotation and with other low-frequency vibrations [8]. Contrarily, dynamics approaches tend to neglect these couplings based on the different time scales involved; usually molecules rotate on a nanosecond time scale whereas the order of magnitude of torsional periods is in the picosecond range. Schemes that employ ultrashort lasers to control molecular processes take advantage of this time scale difference to isolate the torsional degree of freedom. However, the rotation-torsion coupling is built in the initial field-free eigenstates that are not well represented by a direct product of independent rotational and torsional wave functions.

The behavior of nonrigid biphenyl-like molecules subject to an intense laser field is studied here using a rigorous treatment which, unlike previous ones, accounts simultaneously for the large amplitude torsional mode, the overall rotation, and the torsionally mediated interaction with an external electric field. Vibrational modes other than the torsion are neglected. Torsional wave functions of selected rotation-torsion-Stark levels are computed numerically for several strengths of the laser field and for three qualitatively different internal rotation potential energy functions.

Thermal averages of the torsional angle are also evaluated for various temperatures. For two of the three chosen internal rotation potential energy functions, our results indicate that the coupling between overall rotation and torsion is so strong that it makes it impossible to control the internal rotation except for high intensities of the laser field (on the order of  $10^{14}$  W/cm<sup>2</sup>) and for low temperatures (below 5 K). Essentially, it is impossible to localize adiabatically both rings in the same plane. Nonadiabatic processes that could lead to such localized structure cannot be ruled out though.

Our field-free model is based on an old paper by Merer and Watson [9] and involves considering two equivalent planar rigid rings rotating with respect to each other about an axis of internal rotation parallel to the C-C bond. The required coordinates are the three usual Eulerian angles  $\chi$ ,  $\theta$ ,  $\phi$  and the torsional angle  $\gamma$ , with  $0 \leq \gamma \leq 2\pi$ , parameterizing the large amplitude internal rotation of the two rings and such that  $2\gamma$  is the angle of torsion of these two rings. In agreement with Ref. [9], the molecule-fixed axis system is attached to the molecule so that the  $z$  axis is parallel to the axis of internal rotation; the  $x$  and  $y$  axes being parallel to two of the three twofold axes of symmetry. When  $\gamma = 0$  or  $\pi$ , the molecule is planar with all atoms in the  $xz$  plane; when  $\gamma = \pi/2$  or  $3\pi/2$ , the molecule is also planar, but all atoms are in the  $yz$  plane. The rotation-torsion Hamiltonian is built by adding to the torsional Hamiltonian  $H_{\text{tors}}$  given in Eq. (1) of Ref. [9] the  $\gamma$ -dependent rotational Hamiltonian  $H_{\text{rot}}$  given in Eqs. (2) and (3) of this reference. These two operators depend on only two structural constants denoted  $A$  and  $B$ . The molecule is subject to a circularly polarized laser field propagating along the laboratory-fixed  $Z$  axis with laboratory-fixed components  $E_X$  and  $E_Y$  equal, respectively, to  $E \cos \omega t / \sqrt{2}$  and  $E \sin \omega t / \sqrt{2}$ , where  $E$  is the magnitude of the field and  $\omega$  is the laser frequency. Because biphenyl-like molecules have no permanent dipole, the field-matter interaction reduces to the interaction of the electric field with the induced dipole. In the far-off-resonance limit, the operator describing the field-matter interaction becomes  $-\frac{1}{8}(\alpha_{XX} + \alpha_{YY})E^2$ , where  $\alpha_{XX}$  and  $\alpha_{YY}$  are laboratory-fixed diagonal components of the polarizability tensor. This tensor can be evaluated assuming that it is the sum of that of each ring. It can be then conveniently written in the molecule-fixed axis system where its three nonvanishing components are the following:

$$\begin{aligned}\alpha_{xx} &= \alpha_x^0 + \alpha_y^0 + (\alpha_x^0 - \alpha_y^0) \cos 2\gamma \\ \alpha_{yy} &= \alpha_x^0 + \alpha_y^0 + (\alpha_y^0 - \alpha_x^0) \cos 2\gamma \\ \alpha_{zz} &= 2\alpha_z^0\end{aligned}\quad (1)$$

where  $\alpha_x^0$ ,  $\alpha_y^0$ , and  $\alpha_z^0$  are diagonal components of the polarizability tensor of one ring with its atoms in the  $xz$  plane and the axis of internal rotation parallel to the  $z$  axis.

The exact rotation-torsion-Stark field interaction Hamiltonian takes then the following expression:

$$\begin{aligned}H &= AP_\gamma^2 + AJ_z^2 + B_x J_x^2 + B_y J_y^2 \\ &+ \frac{E^2}{8}(\alpha_x^0 - \alpha_y^0) \sin^2 \theta \cos 2\chi \cos 2\gamma \\ &+ \frac{E^2}{8}(2\alpha_z^0 - \alpha_x^0 - \alpha_y^0) \cos^2 \theta \\ &- \frac{E^2}{8}(2\alpha_z^0 + \alpha_x^0 + \alpha_y^0) + V(\gamma),\end{aligned}\quad (2)$$

where  $P_\gamma$  is the momentum conjugated to  $\gamma$ ;  $J_x$ ,  $J_y$ , and  $J_z$  are molecule-fixed components of the rotational angular momentum;  $B_x$  and  $B_y$  are the  $\gamma$ -dependent rotational constants given in Eqs. (3) of Ref. [9]; and  $V(\gamma)$  is the potential energy function for the internal rotation. Like Ramakrishna and Seideman [5], we choose three limiting cases for this function. The potential energy function is assumed to be either zero (Case I), to have four minima at the eclipsed configurations (Case II), or to have 4 minima at the staggered configurations (Case III). Table I gives numerical values for  $A$ ,  $B$ ,  $\alpha_x^0$ ,  $\alpha_y^0$ , and  $\alpha_z^0$  in the case of the biphenyl molecule. These values were used in the remainder of the Letter and were obtained through quantum B3LYP/6-311G( $d, p$ ) correlated calculations at geometries optimized at  $10^\circ$  intervals of the torsional angle. This level of theory has proven successful in describing molecular properties dependent on the internal rotation in biphenyl [10]. Table I also lists expressions for the potential energy function in all three cases. In Cases II and III, the value taken for the height of the hindering potential barrier is  $500 \text{ cm}^{-1}$  as in Ref. [5].

Rotation-torsion-Stark energy levels and eigenfunctions are retrieved accounting for the fact that  $M$  is a good quantum number and that the torsional function is an even or an odd periodic function of the large amplitude coordinate. The matrix of the Hamiltonian in Eq. (2) is first evaluated in a finite basis representation involving cosine or sine torsional functions. It is then transformed into a discrete variable representation [11,12] using the

TABLE I. Numerical values for the five parameters involved in the exact rotation-torsion-Stark field interaction Hamiltonian of Eq. (2) and expressions for the potential energy function.

Parameter	Value <sup>a</sup>	Potential <sup>b</sup>	Case
$A$	0.095 833	$V(\gamma) = 0$	I
$B$	0.016 952	$V(\gamma) = V_4(1 - \cos 4\gamma)/2$	II
$\alpha_x^0 = \alpha_z^0$	11.7	$V(\gamma) = V_4(1 + \cos 4\gamma)/2$	III
$\alpha_y^0$	7.1		

<sup>a</sup>Parameters  $A$  and  $B$  are in  $\text{cm}^{-1}$ , parameters  $\alpha_x^0$ ,  $\alpha_y^0$ , and  $\alpha_z^0$  are in  $\text{\AA}^3$ .

<sup>b</sup>The three internal rotation potential energy functions used in the present calculation. In Cases II and III the height of the barrier is  $V_4 = 500 \text{ cm}^{-1}$ .

orthogonal transformation defined in Eq. (3) of Bačić and Light [11]. Solving Schrödinger's equation reduces then to seeking the eigenvalues and eigenfunctions of the rotation-Stark Hamiltonian for each node value of the large amplitude coordinate  $\gamma$ . These eigenfunctions are then used as basis set functions to solve the torsional problem. The resulting eigenvalues and eigenfunctions are denoted  $E_{M,n}^\Gamma$  and  $\Psi_{M,n}^\Gamma$ , respectively, and are labeled by  $\Gamma$  their symmetry species [9] in  $G_{16}^{(2)}$ , by the quantum number  $M$ , and by a counter  $n$ . In the field-free limit, the usual rotational labels  $J_{K_a, K_c}$  and the torsional quantum number  $\nu_t$  can also be used.

The average value of the square of the torsional function, defined as

$$\langle \delta(\gamma - \gamma_0) \rangle = \int |\Psi_{M,n}^\Gamma(\chi, \theta, \phi, \gamma_0)|^2 d\Omega, \quad (3)$$

was evaluated for several intensities of the laser field and for two  $M = 0$ ,  $A_{1g}^+$  rotation-torsion-Stark levels correlating to the  $0_{00}$  and  $4_{04}$ ,  $\nu_t = 0$  rotation-torsion levels in the field-free limit. The former level is the  $n = 1$  lowest lying level, the latter one is the  $n = 3$  level approximately  $0.34 \text{ cm}^{-1}$  above  $n = 1$  in all three cases. In Case I, in the field-free limit, the average value of the square of the torsional function is nearly constant as expected for  $\nu_t = 0$  free internal rotation levels. Plots of average value of the square of the torsional function can be seen in Fig. 1 for two nonzero intensities of the laser field. When the

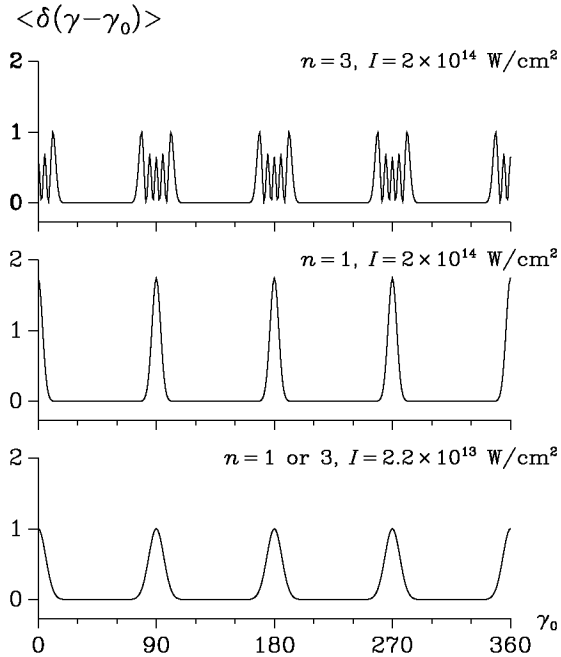


FIG. 1 (color online). In Case I, the average value of the square of the torsional function, as defined in Eq. (3), for the  $M = 0$ ,  $A_{1g}^+$ ,  $n = 1$ , and  $n = 3$  rotation-torsion-Stark levels and for two nonzero intensities of the laser field. For  $I = 2.2 \times 10^{13} \text{ W/cm}^2$ , the same plot should be used for both levels.

intensity of the laser field is  $2.2 \times 10^{13} \text{ W/cm}^2$ , the torsional functions of both levels are almost identical and display four maxima at  $\gamma = 0^\circ, 90^\circ, 180^\circ$ , and  $270^\circ$  corresponding to the planar configurations minimizing the interaction with the electric field. For the highest value of the intensity of the laser field, the torsional functions are also localized around these values of  $\gamma$  but they become quite different. Figure 1 shows that for the  $n = 1$  level, the torsional function still displays four maxima at the same four  $\gamma$  values. For the  $n = 3$  level, a more complicated variation can be seen as the four maxima of the function consist of five close lying peaks; the width of each maximum being about  $30^\circ$ . The qualitative differences between these two levels stem from the fact that the  $n = 3$  level can be coupled to a larger number of high  $\nu_t$ -value levels by the Stark field interaction Hamiltonian as it is characterized by a higher  $J$  value of 4 in the field-free limit. In Case II, for the zero and lowest intensities, the average values of the square of the torsional function display four maxima at  $\gamma$  values equal to  $0^\circ, 90^\circ, 180^\circ$ , and  $270^\circ$  corresponding to the minima of the potential energy function. For the highest intensity, the  $n = 3$  level torsional function displays four maxima that are noticeably broader than for the  $n = 1$  level. This result is quite analogous to the one obtained in Case I and can be understood using the same ideas. The results for Case III are close to those for Case II. For the zero and lowest intensities, the torsional functions display four maxima at  $\gamma$  values equal to  $45^\circ, 135^\circ, 225^\circ$ , and  $315^\circ$  corresponding to the minima of the potential energy function. For the highest intensity, the maxima of the two torsional functions are shifted to the same  $\gamma$  values as for Cases I and II, that is,  $0^\circ, 90^\circ, 180^\circ$ , and  $270^\circ$ . Again, just as for these two cases, the  $n = 3$  level displays broader maxima than the  $n = 1$  level.

For the two levels dealt with in the previous paragraphs and for the same intensity values, Table II gives values for the average  $\langle \cos 4\gamma \rangle$ . This average allows us to estimate how well a level is torsionally aligned as it is nearly 1 for a torsional function displaying four sharp maxima at  $\gamma = 0^\circ, 90^\circ, 180^\circ$ , and  $270^\circ$ . As emphasized by Table II, in all three cases,  $\langle \cos 4\gamma \rangle$  is almost 1 for the highest intensity value and for the  $n = 1$  level. For the other level,

TABLE II. The average value  $\langle \cos 4\gamma \rangle$ , for all three cases, for two rotation-torsion-Stark levels and for three intensities  $I$  of the laser field in  $10^{13} \text{ W/cm}^2$ .

Level	Case	$I = 0$	$I = 2.2$	$I = 20$
$M = 0, A_{1g}^+, n = 1$	I	0.0	0.924	0.974
...	II	0.972	0.974	0.981
...	III	-0.972	-0.943	0.933
$M = 0, A_{1g}^+, n = 3$	I	0.0	0.919	0.775
...	II	0.972	0.974	0.832
...	III	-0.972	-0.962	0.541

this average remains smaller than 0.83 in all three cases indicating that this level is not as well aligned.

In all three cases, with increasing intensity of the laser field, overall angular alignment of the molecule takes place. It is qualitatively similar to the one displayed by a rigid molecule [13] characterized by a polarizability tensor corresponding to the prolate spheroidal case. The present calculation shows that for an intensity of the laser field larger than  $10^{12}$  W/cm<sup>2</sup>, the average value of the squared direction cosine matrix element connecting the laboratory-fixed Z axis and the molecule-fixed z axis,  $\langle\langle \mathbf{i}_Z \cdot \mathbf{i}_z \rangle\rangle^2$ , becomes small for the two levels dealt with in the previous paragraphs in all three cases. Such a result is consistent with the molecule-fixed z axis becoming perpendicular to the direction along which the laser field is propagating in order to minimize the Stark interaction energy.

The thermal average  $\langle\langle \cos 4\gamma \rangle\rangle$  was calculated assuming a Boltzmann distribution of the field-free energy levels and an adiabatic transfer of the population from the field-free to the nonzero field situation. This average was computed in all three cases and for two temperatures. It is plotted as a function of the intensity of the laser field in Fig. 2. For a vanishing laser field and for both temperatures,  $\langle\langle \cos 4\gamma \rangle\rangle$  is as expected zero for Case I. With increasing intensity of the laser field, the thermal average becomes close to 1. This value is reached very rapidly for  $T = 0.1$  K, but more slowly for  $T = 5$  K as the thermal average is only 0.58 for the highest intensity value. In Case II, for a vanishing laser field and for both temperatures,  $\langle\langle \cos 4\gamma \rangle\rangle$  is equal to 1. For  $T = 0.1$  K, with increasing intensity of the laser field, the thermal average remains very close to this value. For  $T = 5$  K, it decreases down to 0.8 for the highest intensity value. In Case III for  $T = 0.1$  K,  $\langle\langle \cos 4\gamma \rangle\rangle$  rises from  $-1$  to 0.83 with increasing intensity of the laser field.

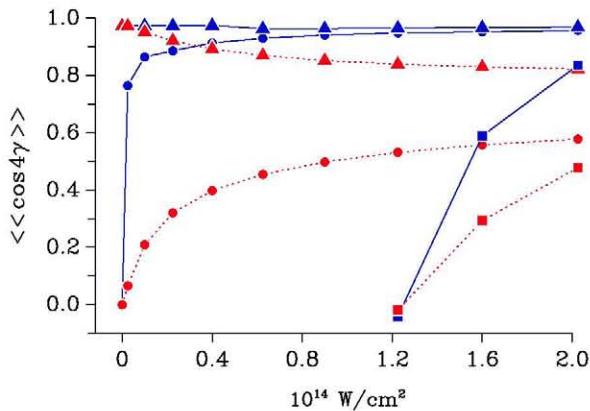


FIG. 2 (color online). Thermal average  $\langle\langle \cos 4\gamma \rangle\rangle$  as a function of the intensity of the laser field for  $T = 0.1$  K (solid line) and  $T = 5$  K (dotted line). The curves corresponding to Cases I, II, and III are plotted with circles, triangles, and squares, respectively. In the last case, only the portion of the curve corresponding to positive values is plotted.

Only the portion of the curve for positive values is shown in Fig. 2. For  $T = 5$  K, the same kind of variation occurs, but the maximum value of the thermal average is only 0.47. Figure. 2 shows that for  $T = 0.1$  K and the highest intensity value, torsional alignment occurs in Cases I and II, but not in Case III. For  $T = 5$  K torsional alignment does not occur in all three cases even for the highest intensity value.

Complexities arising in molecules from strong couplings between large amplitude motions and the overall rotation or other vibrational modes are well known to spectroscopists [8]. We have shown here by using a rigorous theoretical approach that adiabatic control of torsion in biphenyl-like molecules is essentially impeded as rotation-torsion-Stark eigenvectors are heavily affected by such torsion-rotation couplings, that can only be suppressed by an external field for the lowest energy states. Thus thermal averaging prevents localization of the rings on the planar configurations. Therefore we have shown here that the assumption that torsional motions can be isolated from the effects of rotation may prove incorrect.

On the other hand, as shown by Madsen and co-workers [6,7], it is possible to create localized torsional wave packets using more imaginative (and difficult) approaches involving nonadiabatic processes [14] in the ultrafast regime. Also, it should be taken into account that even moderate size molecules like those found interesting for prospective molecular electronics applications present a huge density of vibrational states, including other low-frequency modes, that can be strongly coupled to the torsional states too. These couplings can be another source of problems for the achievement of torsional localization. Thus, the present work suggests that a full understanding of torsional control could require the development of new and sophisticated approaches.

J.O. is grateful to the Spanish Government for the MICINN research Grant No FIS2010-18799.

\*laurent.coudert@lisa.u-pec.fr

†j.ortigoso@csic.es

- [1] H. Stapelfeldt and T. Seideman, *Rev. Mod. Phys.* **75**, 543 (2003).
- [2] K. Horie, H. Ushiki, and F.M. Winnik, *Molecular Photonics: Fundamental and Practical Aspects* (Wiley-VCH, Weinheim, 2000).
- [3] C. Joachin and M. Ratner, *Nanotechnology* **15**, 1065 (2004).
- [4] A. C. Benniston, A. Harriman, P. Li, P. V. Patel, and C. A. Sams, *Phys. Chem. Chem. Phys.* **7**, 3677 (2005).
- [5] S. Ramakrishna and T. Seideman, *Phys. Rev. Lett.* **99**, 103001 (2007).
- [6] C.B. Madsen, L.B. Madsen, S.S. Viftrup, M.P. Jøhansson, T.B. Poulsen, L. Holmegaard, V. Kumarappan, K.A. Jørgensen, and H. Stapelfeldt, *Phys. Rev. Lett.* **102**, 073007 (2009).

- [7] C.B. Madsen, L.B. Madsen, S.S. Viftrup, M.P. Jøhansson, T.B. Poulsen, L. Holmegaard, V. Kumarappan, K.A. Jørgensen, and H. Stapelfeldt, *J. Chem. Phys.* **130**, 234310 (2009).
- [8] J. T. Hougen, *J. Mol. Spectrosc.* **181**, 287 (1997).
- [9] A. J. Merer and J. K. G. Watson, *J. Mol. Spectrosc.* **47**, 499 (1973).
- [10] L. F. Pacios and L. Gómez, *Chem. Phys. Lett.* **432**, 414 (2006).
- [11] Z. Bačić and J. C. Light, *J. Chem. Phys.* **85**, 4594 (1986).
- [12] S. E. Choi and J. C. Light, *J. Chem. Phys.* **92**, 2129 (1990).
- [13] B. Friedrich and D. Herschbach, *Phys. Rev. Lett.* **74**, 4623 (1995).
- [14] T. Seideman and E. Hamilton, in *Advances In Atomic, Molecular, and Optical Physics*, edited by P. R. Berman and C. C. Lin (Academic Press, New York, 2005), Vol. 52, pp. 289–329.